Acta Astronautica 202 (2023) 819–828

Contents lists available at ScienceDirect

Acta Astronautica

journal homepage: www.elsevier.com/locate/actaastro

# GTOC 11: Results from Tsinghua University and Shanghai Institute of Satellite Engineering

Zhong Zhang [a,1], Nan Zhang [a,1], Xiang Guo [a], Di Wu [a,*], Xuan Xie [a], Jinyuan Li [a], Jia Yang [a], Shiyu Chen [a], Fanghua Jiang [a], Hexi Baoyin [a], Haiyang Li [b], Huixin Zheng [b], Xiaowen Duan [b]

[a] Tsinghua University, 100084 Beijing, China
[b] Shanghai Institute of Satellite Engineering, 200240 Shanghai, China

ARTICLE INFO

*Keywords:*
Trajectory design
GTOC 11
Dyson Sphere
Multi-asteroid flyby
Global optimization
Low thrust

ABSTRACT

In this paper, the methods and results from Tsinghua University and Shanghai Institute of Satellite Engineering for the 11th Global Trajectory Optimization Competition (GTOC11) are presented. To deal with the complicated "Dyson Sphere" building problem, a three-stage procedure is conducted. First, the pre-analysis is performed to reduce search space. It is found that two-impulse maneuvers between asteroid flybys are near-optimal, the semi-major axis of the "Dyson Ring" should be better at 1.0–1.5 AU, and the larger arrival mass asteroids tend to be selected. Second, the globally optimal trajectory design problem is further divided into two sub-problems, the mothership trajectory design and the asteroid assignment to the "Dyson Ring" power stations. For the first problem, beam search is used to obtain numerous single mothership trajectories based on a pre-constructed flyby trajectory database of 3–8 asteroids. The overall trajectories and asteroids visited are obtained by selecting 10 mothership trajectories with a genetic algorithm. For the second problem, we build a database of optimal rendezvous times for all the 83,453 asteroids at different phase angles to reach power stations of different radii and phase angles, then a greedy algorithm is proposed to obtain the asteroid arrival schedule based on all the asteroids visited by motherships. Finally, local optimization of asteroid sequence and flyby epochs is conducted. The activation time adjustment in combination with indirect continuous-thrust trajectory optimization is used based on the global optimization result. In the final submission, motherships fly by 388 asteroids, and the minimum mass of twelve power stations reaches 94% of the theoretical upper bound, which is defined using the minimum-time orbital transfers with free initial and target phases.

## 1. Introduction

In the 11th Global Trajectory Optimization Competition (GTOC11) [1], the teams were asked to design the "Dyson Ring" orbit, construct 12 solar power stations in it, and transfer a series of asteroids to these stations. The target of the problem is to maximize the minimum mass of the power stations, minimize the "Dyson Ring" orbit radius, and save the cost (propellant) used by the motherships.

The GTOC11 problem is very complex and involves impulsive and low-thrust trajectory optimization. An attentive analysis provides basic guidelines for the mission design: numerical tests show that the Lambert arcs are optimal solutions in most cases of the asteroid-to-asteroid transfers; The range of "Dyson Ring" location and selection of asteroids can be deduced based on the analysis of a simplified performance index. This part will be introduced in Section 2.

Inspired by the methods for the problems of GTOC 9 [2,3] and GTOC X [4], we develop some practical optimization techniques, such as database generation, local search and greedy approach to improve the computational efficiency or to refine the results. This part will be described in Section 3. In addition, the developed methods include a beam search for constructing single-ship trajectories from an asteroid-chain database, in which the flyby sequences and corresponding epochs have been optimized, a genetic algorithm for selecting 10-ship trajectories, and a greedy algorithm for completing the station assignment problem of asteroids.

The final result submitted for the competition and results of the top ten teams released by organizers are discussed in Section 4. Some conclusions are provided in Section 5.

## 2. Preliminary analysis

Balancing exploration and exploitation is the focus of global optimization. The main objectives of the preliminary analysis are to reduce

* Corresponding author.
*E-mail address:* wud17@mails.tsinghua.edu.cn (D. Wu).
[1] These authors have contributed equally to this work.

https://doi.org/10.1016/j.actaastro.2022.06.028
Received 20 February 2022; Received in revised form 6 June 2022; Accepted 22 June 2022
Available online 24 June 2022

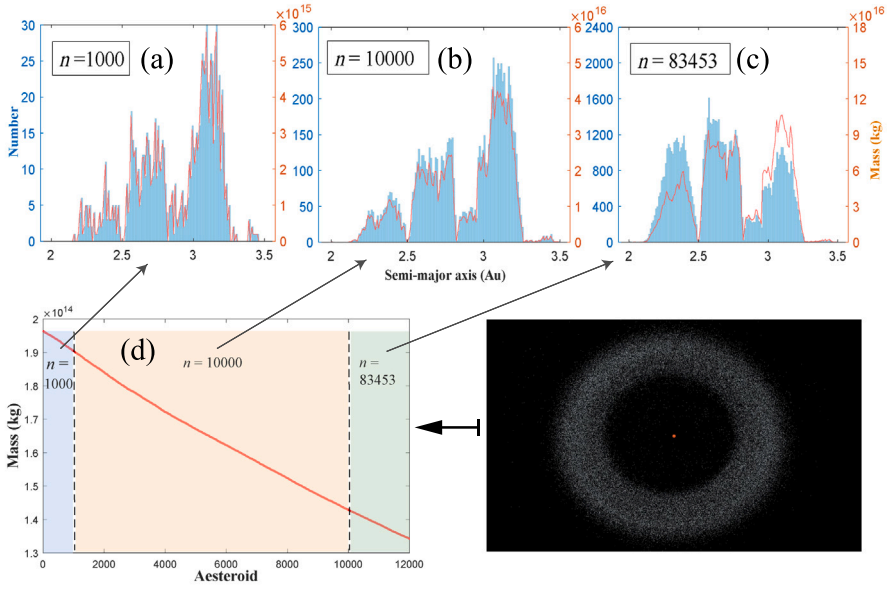


**Fig. 1.** The asteroids distribution and selection. (For interpretation of the references to color in this figure legend, the reader is referred to the web version of this article.)

the global search space and to simplify the specified problem [5]. In the problem formulation, the overall performance index is given as follows:

$$J = B \cdot \frac{10^{-10} \cdot M_{\min}}{a_{\text{Dyson}}^2 \sum_{k=1}^{10} \left(1 + \Delta V_k/50\right)^2} \tag{1}$$

where $a_{\text{Dyson}}$ refers to the semi-major axis of the "Dyson Ring" orbit, $\Delta V_k$ denotes the total velocity increments of the $k$th mothership, $M_{\min}$ refers to the minimal mass among all building stations, and $B$ refers to the bonus factor related to the submitting time.

In this section, an analysis about the three key parameters $(M_{\min}, \Delta V_k, a_{\text{Dyson}})$ of the performance index is carried out, and the conclusions with practical help are then described.

### 2.1. Asteroid distribution and selection

It is nearly impossible to find the globally optimal flyby sequence among all 83,453 asteroids with our current computational capability. Therefore, the main purpose of this subsection is to select the asteroids, as shown Fig. 1. Since the mass of the asteroid is directly related to $M_{\min}$ in the performance index, the analysis of asteroids mass distribution is the primary consideration. In Fig. 1(d), the asteroids are ranked in order of mass from largest to smallest. Among the top 10,000 asteroids, the mass shows a basically linear distribution, and the minimum mass is about 70% of the mass of the largest asteroid. The remaining asteroids (ranked 12,000+) with relatively lower mass are not included in this figure, considering that they have relatively smaller contribution to the performance index even if the mothership flew by them.

The top $n = 1000,\ 10,000,\ 83,453$ asteroids are selected and analyzed in detail as Figs. 1(a), (b) and (c), respectively. The number and mass of the asteroids at each semi-major axis segment (in steps of 0.01 AU between ±0.005 AU) are counted and displayed by the red and blue lines, respectively. As shown in Fig. 1(a) where $n = 1000$, the two lines are close to each other, implying that the masses of all counted asteroids are close (i.e., the total mass of each segment is roughly proportional to the number). This phenomenon is still evident in Fig. 1(b) when the semi-major axis is smaller than 2.5 AU. However, in some segments of Figs. 1(b) and (c), the blue lines are higher than the red lines, meaning that some of the counted asteroid masses are relatively smaller. The top 10,000 asteroids (excluding those with large inclination) are finally selected for the global optimization, and the remaining potential asteroids can be added in the local optimization (Section 3.3). Note that the simulation with the scale of $n = 5000$ has also been conducted, but the results are unsatisfactory, more than 10% worse than the results of $n = 10{,}000$ under the same computational resources. This is supported by the results with $n = 10{,}000$, in which 15% of asteroids are in the mass rank 5000 to 10,000.

### 2.2. Optimal asteroid-to-asteroid impulse number

In this problem, the total mission time is short (20 years). For the flyby trajectory arcs shorter than one revolution, the adjacent asteroids with closer orbits may be transferred at a low cost. From the proximity of orbits, it is assumed that two-impulse is the near-optimal asteroid-to-asteroid impulse number.

A random test scenario is employed to support this hypothesis: Two asteroids are randomly selected from all the 83,453 asteroids, and the departure and arrival epochs are randomly specified in the time interval [30, 360] days. Then, the total velocity increments $\Delta V$ of 2, 3 and 4 impulses are optimized successively. Finally, the $\Delta V$ of the three situations are compared.

After 1000 tests, the two-impulse transfers are optimal in 97% of cases, as shown in Fig. 2. In the remaining 3% of cases, $\Delta V$ is too large to be adopted. Therefore, the asteroid-to-asteroid transfer is solved directly based on Lambert solution in the rest of this study, which is also supported by our final result (Fig. 3).

### 2.3. Optimal semi-major axis range of "Dyson Ring"

The main purpose of this subsection is to determine the range of the optimal "Dyson Ring" radius. To simplify the distribution of the asteroids, we assume that they move in coplanar circular orbits, their orbit radii are distributed discretely (step of 0.05 AU), and the asteroid mass for each radius is the sum of the asteroid masses in the radius range ±0.025 AU. So, the departure orbit is defined to represent the asteroid orbits around it. That is, it is assumed that all asteroids around the departure orbit are located on this departure orbit.

To consider the effect of $a_{\text{Dyson}}$ comprehensively, the estimated performance index is defined as:

$$J^* = \frac{1 - \alpha \Delta t}{a_{\text{Dyson}}^2} M \tag{2}$$

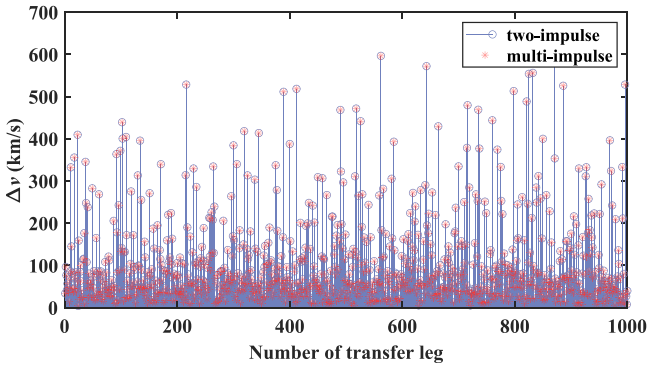


**Fig. 2.** Two-impulse vs. multi-impulse in random asteroid transfer.

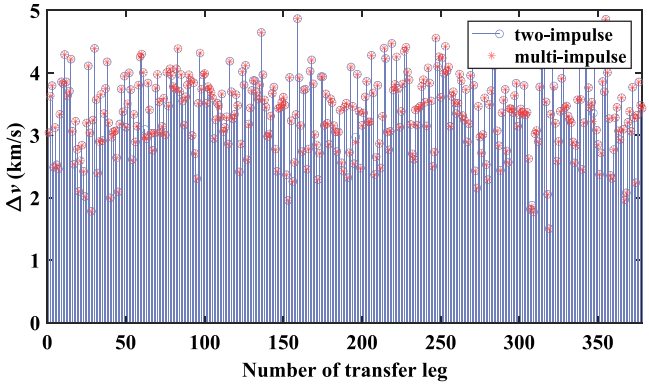


**Fig. 3.** Two-impulse vs. multi-impulse in final result.

where $M$ is the total mass of the asteroids around the departure orbit, and $1-\alpha\Delta t$ refers to the mass decay ratio obtained by solving an optimal transfer problem from the departure orbit to the "Dyson Ring" orbit. Here, the mothership trajectory is not considered, such that the departure orbit and the total mass can be simply estimated.

The minimum transfer times from the departure orbits at 1.0–3.5 AU to the "Dyson Ring" orbits at 1.0–3.5 AU are calculated separately, and every estimated performance index is further calculated and shown in Fig. 4. The indirect method is used to solve the orbital transfer problem between two circular orbits. Each curve represents the estimated performance index for reaching different "Dyson Ring" radii from one departure orbit, and each peak shows the corresponding optimal "Dyson Ring" radius. It shows that each curve displays maximum values at 1.0–1.2 AU and 1.3–1.5 AU. So, it is concluded that the optimal "Dyson Ring" radius is between 1.0 and 1.5 AU.

## 3. General description of the method

This section will describe the optimization methods developed for the submitted results. The problem of successive flybys of multiple asteroids is a classical problem in GTOCs, while that of "Dyson Ring" construction is relatively new. So, the globally optimal trajectory design problem is further divided into two sub-problems: 1. motherships trajectory design; 2. asteroids assignment to the "Dyson Ring" power stations.

The first subproblem optimizes the asteroids-flyby sequence of the motherships and corresponding flyby epochs. The second subproblem optimizes the orbital elements of the "Dyson Ring", construction time window of each station, and assignment of asteroids, based on the visited asteroids obtained by the first subproblem.

The end of this section will describe how to combine all the methods to solve the final problem.

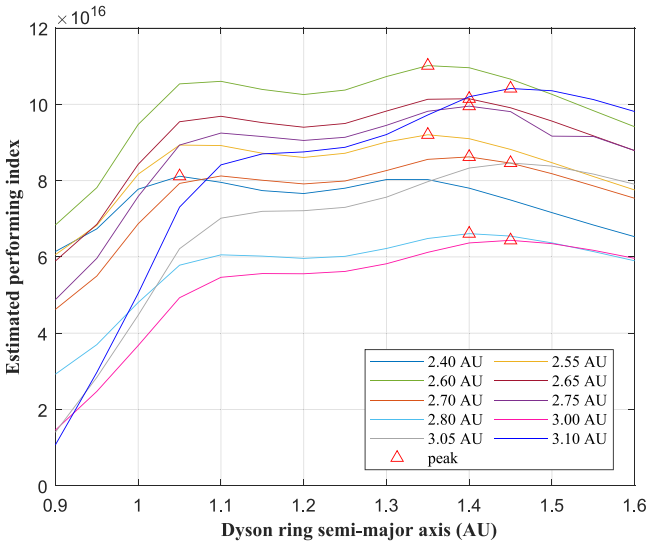


**Fig. 4.** The optimal semi-major axis range of Dyson Ring.

### 3.1. Trajectory design of motherships

#### 3.1.1. Handling flyby constraints

For the constraint that relative velocity is less than 2 km/s at flyby time, how to further decrease the velocity increment while satisfying the flyby constraint is the key to optimization. An approach is proposed to solve this by directly using the rendezvous case first and then correcting the velocity increment with a geometric method. Solving the rendezvous problem is technically simpler since there is no need to optimize the flyby velocity, thus reducing the optimization state space. The method of correcting velocity increment only considers the arrival velocity $\boldsymbol{V}_1$ of the previous transfer, the departure velocity $\boldsymbol{V}_2$ of the next transfer and the asteroid velocity $\boldsymbol{V}_0$ at the rendezvous time. The geometric schematic is shown in Fig. 5, where $\boldsymbol{V}_1$ and $\boldsymbol{V}_2$ are given based on the Lambert problem described in Section 2. As can be seen from Fig. 5, in speed space, $D$ and $E$ denote the endpoints of $\boldsymbol{V}_1$ and $\boldsymbol{V}_2$, respectively, and any point $P(\boldsymbol{V}_0')$ in the sphere (with the point $O(\boldsymbol{V}_0)$ as the center and the maximum relative velocity $R = 2$ km/s as the radius) satisfies the flyby constraint. The objective is to minimize the total velocity increment $|\Delta\boldsymbol{V}_1| + |\Delta\boldsymbol{V}_2|$, i.e., $\min \left|\overline{DP}\right| + \left|\overline{PE}\right|$.

Now, this physical problem can be described as the following mathematical problem: Given two fixed points $D$ and $E$ and a sphere $O$ in a three-dimensional Euclidean space, find a point $P$ in the sphere $O$ such that it has the shortest distance $\left|\overline{DP}\right| + \left|\overline{PE}\right|$ to the two points. This three-dimensional problem can be further degraded to a planar problem, where $P$ is on the plane $DEO$ determined by point $D, E,$ and $O$. (Since the point $P'$ can be obtained from the projection of the point $P$ to the plane $DEO$ if $P$ is not on this plane, while $\left|\overline{DP'}\right| + \left|\overline{P'E}\right| < \left|\overline{DP}\right| + \left|\overline{PE}\right|$.)

Only two cases of the plane geometry problem need to be categorized and discussed: 1. When the line segment $DE$ intersects the circle $O$: Point $P$ can be any point in the $AB$ line segment of the intersection point. If $D$ or $E$ is in (on) the circle, then $A$ or $B$ degenerates into $D$ or $E$ accordingly. 2. When the line segment $DE$ is separated from the circle $O$: For all points on the eclipse in the plane, the sum of the two distances to the focal points $D, E$ is constant $2a$. If the semi-major axis $a$ of the ellipse keeps increasing until it is tangent to the circle $O$, it is easy to conclude that the sum of distances is the shortest. The point $P$ is the tangent point of the circle and the ellipse. Since point $P$ satisfies the ellipse equation, the circle equation, and the equation of the same tangent line slope between the ellipse and the circle at $P$, the above three equations (the unknown quantities are the semi-major axis $a$ and

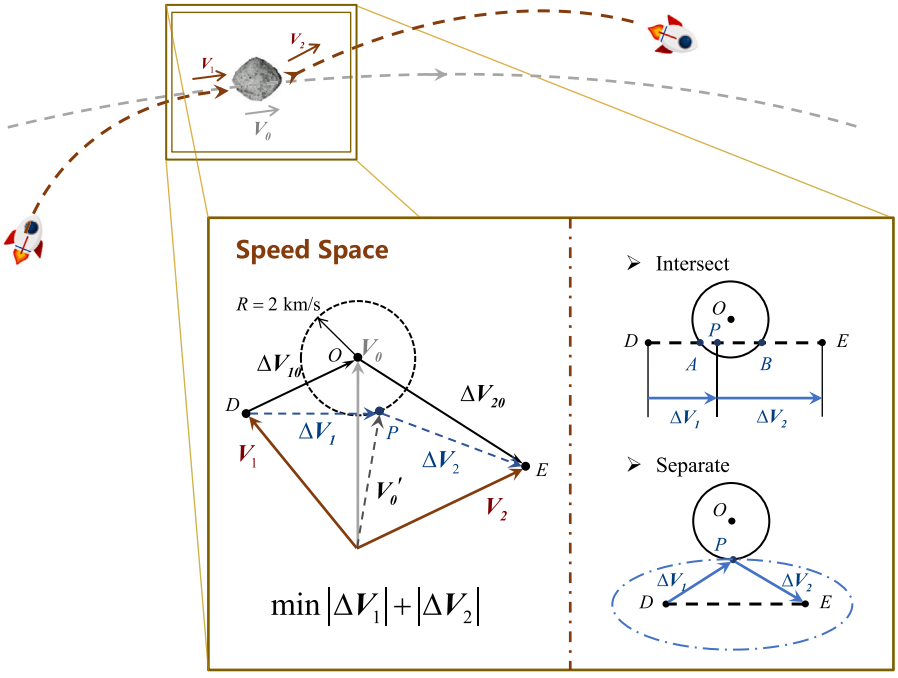


**Fig. 5.** Geometric method of handling flyby constraints.

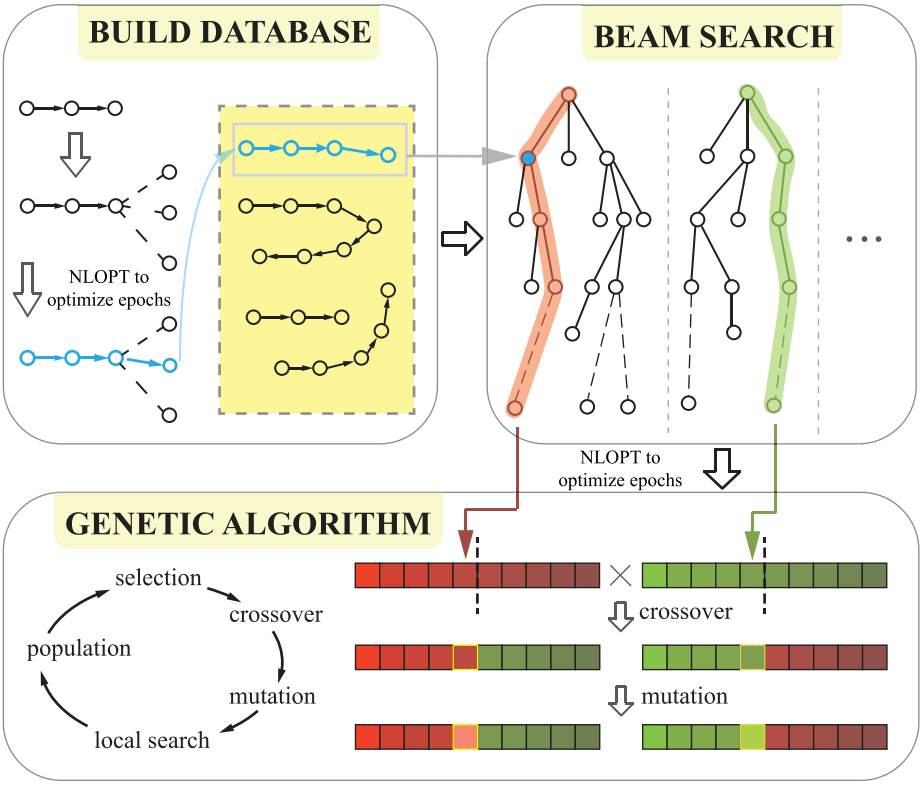


**Fig. 6.** Schematic diagram of mother ships trajectory design.

the two coordinates of point $P$) can be combined to obtain a quartic equation. Point $P$ can be determined by the analytical root formula of the quartic equation.

### 3.1.2. *Asteroid chain building*

Before the global optimization begins, a database is built and called the "asteroid-chain" database, as shown in Fig. 6. Each asteroid-chain contains the sequence and flyby epochs of 3–8 asteroids, and the average velocity increment and time interval of each asteroid-to-asteroid leg is about 0.46 km/s and 150 days, respectively. The reason for building this database is that optimizing the flyby epochs significantly reduces the velocity increment, while this procedure is too computationally demanding to be executed multiple times [6].

The steps to build this database are summarized as follows:

First, a database called "candidate asteroid" is created based on the numerically calculated transfer velocity increments between all asteroids (10,000). This step is to avoid wasting computation resources on those unpromising asteroids, and the second step will optimize flyby epochs to reduce the velocity increment. Some specific parameters are set as follows: departure epochs from 0 to 6000 days with step 40 days, and transfer intervals from 40 to 360 days with step 40 days. If the transfer velocity increment from asteroid A to B is less than 2000 m/s, asteroid B is regarded as a candidate asteroid for asteroid A and will be stored in candidate asteroid database. Thus, this candidate asteroid database can provide a list of candidate asteroid IDs with the inputs of asteroid ID, departure epoch, and transfer interval.

Second, the $(i+1)$-asteroid-chain is generated based on $i$-asteroid-chain and candidate asteroid database. Starting from every final point of $i$-asteroid-chain, the subsequent asteroids given by "candidate asteroids database" are traversed, and the flyby time is first traversed discretely and then optimized with a local optimizer after handing the flyby constraints. Here, $i$ denotes the asteroid chain with $i$ asteroids. To create a $(i+1)$-asteroid-chain, the flyby epochs (size $i+1$) of all asteroids in this chain are optimization variables. The first to $i$th initial values for the local optimizer are provided by previous epochs stored in the chain, and the last asteroid flyby epoch is traversed (transfer time interval from 3 to 165 days with step 3 days), and the optimization objective is the minimum total velocity increment. The velocity increment is first computed under the rendezvous case and then adjusted to the flyby case, where $\boldsymbol{V}_1$ and $\boldsymbol{V}_2$ of the second asteroid to the $i$th asteroid are refined according to Section 3.1.1. Note that the initial asteroid chains ($i$=1) contain all asteroids (10,000) with flyby epochs from 0 to 6480 days with step 8 days. The local optimizer is a nonlinear programming open-source algorithm library called NLOPT [7], where the specific nonlinear programming algorithm chosen is Sbplx [8], an optimization algorithm that does not require user-supplied gradients.

Finally, if the velocity increment and transfer time are less than the given thresholds, they are placed in the $(i+1)$-asteroid-chain database; otherwise, they are discarded. The threshold values are given manually. Naturally, if the thresholds are high, the database will be too large, and the database will not work well if too low. We ended up with a reasonably sized database by manually adjusting the thresholds. The final asteroid-chain database contains about 60,000,000 ($10,000,000\times6$, $i$ from 3 to 8) asteroid chains, i.e., there are about 6000 asteroid chains starting at each asteroid (10,000) on average.

#### 3.1.3. Connecting chains to single-ship trajectory

Each "asteroid-chain" is connected as a node in the traditional beam search [9] to complete a single mother ship trajectory. A brief beam search procedure is as follows: Before the tree search, the 2400 best first-asteroid-chains, i.e., root nodes, are determined by traversing all the 60,000,000 asteroid chains departing from Earth; Then, the beam search is performed starting from different first-asteroid-chains (2400 times). During the expansion phase, the last asteroid is used as input to obtain asteroid list from the candidate asteroid database. With each candidate asteroid as starting one, asteroid chains satisfying the time constraint are expanded; Finally, each node is computed the heuristic index and the first $W$ nodes are selected for the next layer, where $W=2000$ is the beam width. The single-ship trajectory is stored when the node reaches the stopping criterion.

Here, the heuristic function of the following form is defined:

$$h_e = \frac{m_{\text{total}}}{\Delta V^{\varepsilon}\left(t_f - t_0\right)^{\gamma}} \tag{3}$$

Where $m_{\text{total}}$ refers to the total asteroid remaining mass that mothership flies by, $\Delta V$ refers to the total velocity increment that mothership consumes, $t_0, t_f$ refer to the departure epoch of mothership and the flyby epoch of the current last asteroid, $\varepsilon, \gamma$ refer to the design parameters and are set to around 0.6 and 0.3, respectively. The units of variables in the heuristic function are normalized, that is, the length unit is normalized to 1 AU, the time unit is normalized to $1/(2\pi)$ year, and the constant of sun gravitational are normalized to 1. This exponential performance index of heuristic function tends to have a solution better than the original performance index. The reason is that the exponential form is more intuitive to show the impact of different parameters on the variation of the heuristic function. It is also easier to construct a uniform format in different problems. This phenomenon was first noticed in [10] and is further verified in GTOC 11 problem.

The node expansion is stopped when the heuristic function no longer grows or when the last asteroid cannot reach the "Dyson ring", and the beam search is stopped in sync with the node expansion. As a result, plenty of single-ship trajectories are obtained. These trajectories will be further optimized flyby epochs by NLOPT [7] and evaluated by a single-ship performance index $J_{\text{single}}$. Only those trajectories ($J_{\text{single}} > 12$) will be stored, and the final number of stored single-ship trajectories is 359,216. $J_{\text{single}}$ is defined as:

$$J_{\text{single}} = \frac{10^{-14}\cdot m_{\text{total}}}{(1+\Delta V/50)^2} \tag{4}$$

#### 3.1.4. 10-Ship trajectories combination

In this subsection we explain how to select the best 10 mothership trajectory combination from all single-ship trajectories produced from beam search ($C^{10}_{359,216}$ chances). A custom genetic algorithm (GA) with local search is adopted. In the GA, a chromosome gene is represented as one single-ship trajectory obtained by the beam search, and the integer encoding (between 1 and 359,216) is used. One chromosome consists of 10 genes, and the $k$th gene means the $k$th mothership trajectory. The fitness function is set to the performance index (see Eq. (1)), where $M_{\text{min}}$ is estimated by a greedy algorithm, which will be introduced in Section 3.2.3.

The way of crossover and mutation is classic, as shown in Fig. 6. If multiple chromosomes are identical in the new generation, only one is preserved, and the others are regenerated randomly. A local search method is used for all the chromosomes in the new population: try each feasible gene and replace the original gene with others for the highest index. If two or more motherships fly by the same asteroid more than once, the corresponding trajectory is randomly removed until the constraint is satisfied.

The GA is terminated when the maximum number of iterations is reached. The population size, crossover rate, mutation rate, and terminating generations are set to 128, 0.9, 0.2, 10, respectively.

The global optimization results produced by GA will be further locally refined, which will be introduced in Section 3.3. The greedy algorithm, which will be presented in Section 3.2.3 and can provide the asteroid arrival schedule and the resulting estimated $M_{\text{min}}$, is called as a subroutine in the calculation of the GA fitness function. A more comprehensive summary of optimization methods is included in Section 3.4.

### 3.2. Asteroid assignment to the "Dyson Ring" power stations

#### 3.2.1. Indirect method

As requested in the problem, once the ATD on the asteroid is activated, the asteroid will consume its own mass and transfer to the target station with a fixed magnitude of acceleration. So the shorter the transfer time, the greater the remaining mass of the asteroid when it reaches the target station, and therefore the final performance index will be higher. The transfer process of each asteroid can be regarded as a time-optimal rendezvous problem with constant acceleration, which can be solved by the indirect method and the objective function is given as

$$J = \lambda_0 \int_{t_0}^{t_f} 1\mathrm{d}t \tag{5}$$

where $\lambda_0$ is a positive scaling factor that does not change the origin optimal control problem [11], and $t_0$ and $t_f$ are the initial and rendezvous times, respectively.

The modified equinotical elements (MEE; $p$, $e_x$, $e_y$, $h_x$, $h_y$, $L$) are chosen to represent the orbital states in our method because they are nonsingular, efficient, and robust [12,13]. The relationship between MEE and the classical orbital elements is expressed as

$$\begin{array}{lll} p = a(1-e^2) & e_x = e\cos(\omega+\Omega) & e_y = e\sin(\omega+\Omega) \\ h_x = \tan(i/2)\cos\Omega & h_y = \tan(i/2)\sin\Omega & L = \omega+\Omega+f \end{array} \tag{6}$$

where $a$ is the semi-major axis, $e$ is the eccentricity, $i$ is the inclination, $\Omega$ is the right ascension of the ascending node, $\omega$ is the perigee anomaly, and $f$ is the true anomaly.

Since the magnitude of acceleration is fixed, the mass of the asteroid will not affect its motion and can be neglected in the motion equations. Defining the state vector as $\boldsymbol{x} = [p, e_x, e_y, h_x, h_y, L]^{\mathrm{T}}$, the dynamic equations with constant acceleration magnitude $a$ can be written as

$$\dot{\boldsymbol{x}} = a\boldsymbol{M}\boldsymbol{\beta} + \boldsymbol{D} \tag{7}$$

where $\boldsymbol{\beta}$ is the unit vector of the thrust direction, $\boldsymbol{M}$ is a transformation matrix, and $\boldsymbol{D}$ is the gravity vector. The detail expressions of $\boldsymbol{M}$ and $\boldsymbol{D}$ can be found in [14].

The indirect method is currently one of the most accurate methods to solve the trajectory optimization problem. By introducing the costate vector $\lambda_x(t)$, the Hamiltonian is built as

$$H = \lambda_x \cdot \dot{\boldsymbol{x}} + \lambda_0 = a\lambda_x^{\mathrm{T}}\boldsymbol{M}\boldsymbol{\beta} + \lambda_x^{\mathrm{T}}\boldsymbol{D} + \lambda_0 \tag{8}$$

According to Pontryagin's minimum principle (PMP), the Hamiltonian needs to be minimized, so the optimal thrust direction is determined by

$$\boldsymbol{\beta} = -\frac{\boldsymbol{M}^{\mathrm{T}}\lambda_x}{\|\boldsymbol{M}^{\mathrm{T}}\lambda_x\|} \tag{9}$$

and costate differential equations are given by

$$\dot{\lambda}_x = -\frac{\partial H}{\partial \boldsymbol{x}} = -a\frac{\partial(\lambda_x^{\mathrm{T}}\boldsymbol{M}\boldsymbol{\beta})}{\partial \boldsymbol{x}} - \frac{\partial(\lambda_x^{\mathrm{T}}\boldsymbol{D})}{\partial \boldsymbol{x}} \tag{10}$$

For rendezvous problems, the state variables must satisfy the following boundary conditions:

$$\boldsymbol{x}(t_0) = \boldsymbol{x}_0, \quad \boldsymbol{x}(t_f) = \boldsymbol{x}_f \tag{11}$$

With reference to the transversality conditions in [15], the optimal arrival time $t_f$ is determined by

$$H(t_f) - \lambda_x(t_f)\cdot\dot{\boldsymbol{x}}_f = 0 \tag{12}$$

As demonstrated in [16], the Lagrange multipliers are defined as $\lambda \triangleq [\lambda_0; \lambda_x(t)]$ and $\lambda(t_0)$ can be normalized to reduce the solution space, viz.

$$\|\lambda(t_0)\| = 1 \tag{13}$$

So far, the optimal control problem can be transformed into a two-point boundary value problem (TPBVP), and the shooting function is given as

$$\boldsymbol{\Phi}\left[\lambda(t_0); t_f\right] = \begin{bmatrix} \boldsymbol{x}(t_f) - \boldsymbol{x}_f \\ H(t_f) - \lambda_x(t_f)\cdot\dot{\boldsymbol{x}}_f \\ \|\lambda(t_0)\| - 1 \end{bmatrix} = \boldsymbol{0} \tag{14}$$

which can be solved by the shooting method [17]. Once Eq. (14) is solved and $\lambda_x(t_0)$, $t_f$ are obtained, Eq. (7) and (10) can be integrated again to get the states and control laws of the whole transfer process. Meanwhile, the remaining mass of the asteroid can be computed as

$$m^{\mathrm{ast}}(t_f) = m_0^{\mathrm{ast}} - \dot{m}\cdot(t_f - t_0) \tag{15}$$

#### 3.2.2. Low-thrust rendezvous database and transfer time prediction

The indirect method takes about 0.1 s to calculate the minimum transfer time for each rendezvous from the asteroid to the power station with the above processing. However, this computational speed is insufficient to support the global optimization. Some estimation methods of the transfer times, such as the Edelbaum's method [18] or the shape-based method [19,20], do not meet the high accuracy required for this problem (The required relative accuracy can be roughly calculated as follows. It usually takes about 1000 days to push most visited asteroids to arrive at the power station. The estimated transfer time absolute error should be less than the real transfer time difference between fifteen phase degrees, which is generally 10 days in this problem. So, the relative error is about 1%). Deep learning perhaps is a solution [21], but the process of training the network and tuning the parameters may take a while. Therefore, a low-thrust rendezvous database was created to provide the minimum transfer time prediction for all asteroids to rendezvous with different stations at any given moment.

The parameters of the database are as follows: Asteroids (83453 options); departure true anomaly, 0 to 345 degrees, steps of 15 degrees (24 options); "Dyson Ring" radius, 0.8 to 2.0 AU, steps of 0.05 AU (25 options); station phase angle, 0 to 345 degrees, steps of 15 degrees (24 options). The inclination angle of "Dyson Ring" is assumed to be zero. Note that the optimal transfer time for each asteroid to reach different "Dyson Ring" orbits (phase-angle-free) is also built into a low-thrust transfer database, which can be used to estimate the minimum time of the rendezvous and the maximum asteroid arrival mass. With large amounts of data, fast storage and reading techniques are also considered: the database in integer data structure is then converted to binary, with a final size of about 4.5 GB.

Through the low-thrust rendezvous database, a subroutine is used to estimate the minimum time of flight with the inputs of asteroid ID, departure true anomaly, "Dyson Ring" radius, and station phase angle. This estimated time is obtained by three-dimension linear interpolation (using $2\times2\times2 = 8$ data grids) for the mentioned last three inputs.

#### 3.2.3. Asteroid arrival schedule algorithm

This subsection is to solve the second subproblem in global optimization, i.e., how to identify the orbital parameters of "Dyson Ring", station construction time interval, phase angles of stations, and asteroid arrival schedule when all visited asteroids and their flyby epochs are obtained. A novel, greedy algorithm is proposed to solve this problem partially.

As mentioned in Section 3.1.4, the greedy algorithm provides an estimated $M_{\min}$ for the GA fitness function ($J$), which will be executed multiple times. So, there is a trade-off between the efficiency and effectiveness of this algorithm. As a result, the inputs to the greedy algorithm are all visited asteroids and their flyby epochs, the orbital parameters of "Dyson Ring", and the station construction time interval. On the other hand, the outputs are the phase angles of stations, asteroid arrival schedule and $M_{\min}$. That is to say, the last two inputs are given manually after several trials and can be further optimized in Section 3.3. This processing speeds up the greedy algorithm operation, and it takes 0.1 s per execution.

This algorithm aims first to determine the phase angle of stations from the late-arrival asteroids and then adopt subsequent local search to complete the asteroid assignment. Let us explain this in more detail. The later the asteroid is flown over by the mothership, the less choice of power stations the asteroid can reach. To make each visited asteroid reach the power station successfully, the algorithm takes the late-arrival asteroids to determine the phase angles of the late-built station. The following is an example of how to determine the phase angles of the latest built station and the same for other station phase angles determination. Those asteroids that can only reach the latest built station are classified in a group. All possible station phase angles are traversed by this group of asteroids, and the one with the maximum mass will be greedily chosen. And all these asteroids are temporarily assigned to this station. When all phase angles are finalized, the local search is used to adjust some asteroid assignments to make the minimum station mass increase.

The pseudo-code of the algorithm is shown in Fig. 7. A schematic diagram of this greedy algorithm is also provided for the explanation, as shown in Fig. 8. Note that the phase angles of stations and asteroid departure true anomaly are considered only as provided by the low-thrust rendezvous database.

**Input**: visited asteroids and their flyby epochs, orbital parameters of "Dyson ring", and station construction time interval
Sort the visited asteroids according to the time of arrival epoch (phase-angle-free)
Group asteroids (1-12) in chronological order
**for** the *i* th station from the last to the first station
  **for** feasible phase angle
    **for** all the last asteroids in group *i* to 12
      Calculate the optimal transfer time
      If reachable, add the asteroid arrival mass
    **end for**
    Record the mass of this station
  **end for**
  Select the phase angle corresponding to the maximum mass station
  Determine the phase angle and asteroids to reach the *i* th station
**end for**
Local search: Enum all the allocated asteroids in other stations to move to the minimum mass station, and select the asteroid with the largest total mass of the station. Repeat the process until mass of the minimum mass station no longer increases.
**Return:** phase angles of stations, asteroid arrival schedule and $M_{min}$

**Fig. 7.** Pseudo-code of the greedy algorithm.

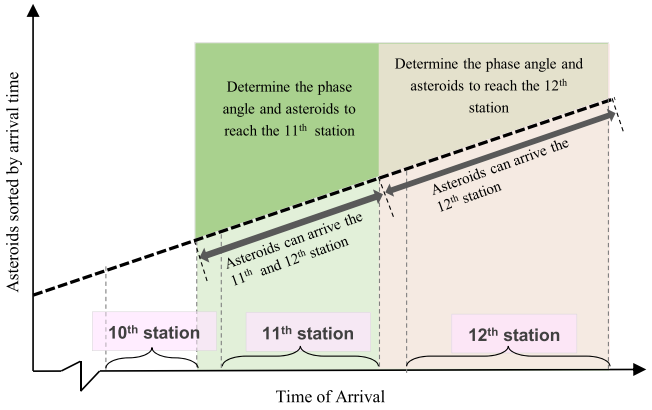


**Fig. 8.** Determination of the station phase angle in the greedy algorithm.

### 3.3. Local optimization

This section presents some practical techniques for the subsequent local optimization, based on the results already obtained by the global optimization. Eventually, the local optimization can increase the performance index by nearly 10%.

#### 3.3.1. Adjustment of the asteroid-flyby sequence

In the local optimization, a subroutine of local search is proposed to adjust the asteroid-flyby sequence by employing add, delete, and swap operators in turn. The illustration of these operators is shown in Fig. 9, and this part is inspired by Ref. [3]. After the sequence has been adjusted, the flyby epochs of visited asteroids are further optimized using the NLP [7], where the characteristic of NLP is consistent with that presented in Section 3.1.2. This subroutine continues until the stopping iteration is met or a better score cannot be found. It usually results in removing asteroids that cannot reach the power stations and adding some remaining asteroids at low-velocity increment cost. This step finally increase the performance index about 500 points.

#### 3.3.2. Adjustment of "Dyson Ring" orbit and station construction time

As mentioned earlier in Section 3.2.3, orbital parameters of "Dyson Ring" and station construction time interval in the input of greedy algorithm are manually given. In this step, these variables are further optimized. The particle swarm optimization (PSO) algorithm is used

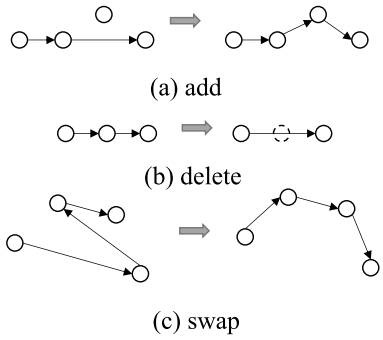


**Fig. 9.** Illustration of local search operators.

to optimize the station construction time window. The optimization variables for the PSO are the 12-station construction durations, each of which ranges from 0 to 540 days. The construction end epoch of the last station is the end of the mission (103044 MJD), and the duration between two successive building stations is set to 90 days. The PSO swarm size and the iteration number are 128 and 1000, respectively. The adjustment of the "Dyson Ring" orbital elements is obtained by building a fine-grained database: Only visited asteroids are considered; The inclination and RAAN are determined by the average orbital angular momentum of the visited asteroids; The step size of the semi-major axis is reduced to 0.01 AU from the original value (i.e., 0.1 AU).

Before outputting the final low-thrust trajectory, the departure epoch of each asteroid is traversed around the estimated departure epoch that is produced by the greedy algorithm. The optimal departure epoch with the maximum arrival mass is adopted for output. This step is to prevent the selection of the initial guesses from leading to local optima, and to decrease the effect of transfer time estimation error by the low-thrust rendezvous database. This subsection raise the performance index by about 200 points.

### 3.4. Summary of the optimization method

Finally, a summary of the developed methods is presented in a flowchart, as shown in Fig. 10. At the very beginning of the competition, we analyzed the problem based on the performance index and drew three practical conclusions. That is to say, two-impulse maneuvers between asteroid flybys are near-optimal; semi-major axis of the "Dyson Ring" should be better at 1.0–1.5 AU; the asteroids with larger final arrival mass tend to be selected for the global optimization. These conclusions deepen our understanding of the problem, which is further simplified with a reduced global search space.

In the global optimization, the problem is divided into two subproblems: the trajectory design of motherships and the asteroid assignment to the "Dyson Ring" power stations. Based on the characteristics of each subproblem and the need of high efficiency, a series of specific databases are built, to allow for the fast solution of some fundamental problems. The database establishment is the most computationally demanding step.

From there, we use beam search together with a genetic algorithm to solve the first subproblem and a greedy algorithm to solve the second one. These two subproblems were at first studied independently and were then coupled. The total arrival mass in the BS heuristic function is estimated by the transfer time, and the $M_{min}$ for the GA fitness function is provided by the greedy algorithm. In order to get a fast and viable solution, the methods used are based on adaptations of well-established codes. Then, the local optimizations adjusted on top of the existing results and improved the final performance index by nearly 10%.

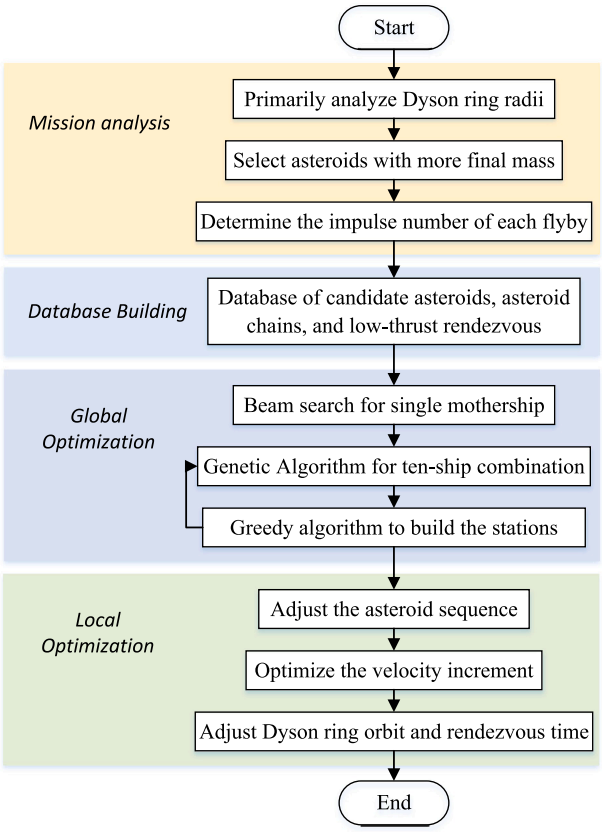


**Fig. 10.** The flow chart of general method.

## 4. Results

In this section, our final submission results are presented in detail. The analysis to the results of the top 10 teams is also conducted. All programs that require computational resources are performed on a cluster of supercomputers and the C++ platform, each node running on an AMD EPYC 7H12 processor with 128 threads at 2.6 GHz. Of all algorithms covered in the article, only NLP [7] and shooting method [17] are provided by other parties. Other algorithms such as BS, GA, and PSO are our custom versions, but most of them are based on their legacy versions, and the modifications are described in their corresponding sections.

The total computation wall-clock time is as follows: During the database generation stage, the asteroid-chain database used 1 node and computed for 2 days; the low-thrust database used 3 nodes and computed for 3 days each time. This database was updated 3 times to avoid the local optima of the indirect method. During the optimization stage, both the beam search and genetic algorithms used 1 node and computed for 2 days; local optimization used 1 node and computed for 1 day.

### 4.1. Winning results

The final submission results are as follows, ten motherships flew by 388 asteroids with an average velocity increment of 16.6 km/s per ship. The radius of "Dyson Ring" is at 1.10 AU, and $M_{\min}$ is $1.814\times10^{15}$ kg. The difficulty of mothership trajectory design is how to fly by as many asteroids as possible with velocity increment low enough. Due to the tremendous search space of the problem, our existing techniques cannot optimize the flyby sequence while optimizing the specific flyby times very well in the global search. Instead, we ended up building the asteroid-chain database and splicing asteroid-chains to achieve the final mothership trajectories. Note that the flyby epochs in asteroid-chain are optimized when building the database. A complete summary of the final submitted solution is provided in Fig. 11 and Table 1, where $T_k^s$ refers to the departure epoch of the $k$th mothership from the Earth, and $n$ refers to the flyby asteroid number by each mothership.

### 4.2. Results of top 10 teams

The detailed information of the top 10 teams is summarized in Table 2, where those results marked with a star are calculated by our program, and the rest are released by the organizer. The range of "Dyson Ring" semi-major axis distribution for the top 10 teams confirms our pre-analysis. It seems that only the top three teams had optimized the other "Dyson Ring" orbital elements (the inclinations of the 9th and 10th teams seem to be too large). In addition, the table allows analyzing the performance of each team's mothership trajectory and asteroid assignment. The theoretical upper bound of $M_{\min}$ is calculated by the sum of maximum mass divided by 12, and the maximum mass (i.e., the minimum arrival time) can be obtained by directly calculating the minimum time for the asteroid to reach the "Dyson Ring" orbit (neglecting the initial and final phase angles). This leads to the calculation of the dividing station efficiency, as shown in the third last row of the table. It can be seen that most of the top 10 teams can achieve more than 80% efficiency, and the top 2 teams can achieve 90%. Combining the mothership trajectories of each team with our greedy algorithm yields the estimated scores in the table, which means that they can be used to evaluate the mothership trajectories separately. Note that among the parameters of the greedy algorithm, the "Dyson Ring" radius is based on each team's result, while the inclination angles are all assumed to be zero. The construction time windows are still given manually, the same as we used in the global optimization. The larger estimated score (the second last row of Table 2) means that the mothership trajectories are better and more likely to end up with better results. Our final submitted result is higher than our estimated score because of the adjustment of "Dyson Ring" orbit and station construction time (Section 3.3.2).

## 5. Conclusions

The flyby of multiple asteroids and the construction of the "Dyson Ring" skillfully combine the impulsive and low-thrust trajectory design in a challenging and interdependent combinatorial optimization problem. Some experimental efforts by our team during GTOC11 may provide some insights: Solving the rendezvous problem in combination with the geometric corrections when the relative flyby velocity is constrained; Optimizing the flyby times to construct the asteroid chains to deal with the time-dependent problems in advance, especially when the global search space is vast; An exponential form of the heuristic function in beam search seems to achieve a better score than the original form; When the analytical model is not good enough, a low-thrust solution database is constructed to obtain accurate rendezvous time interval.

## Declaration of competing interest

The authors declare that they have no known competing financial interests or personal relationships that could have appeared to influence the work reported in this paper.

## Acknowledgments

The TsinghuaLAD&509 team thanks the organizers of GTOC11: National University of Defense Technology and Xi'an Satellite Control Center, for posing such a comprehensive and futuristic problem, and for making the logistics of low-thrust trajectories solution verification trivial.

This work is supported by the National Natural Science Foundation of China (Grant number 12022214, U21B2050).

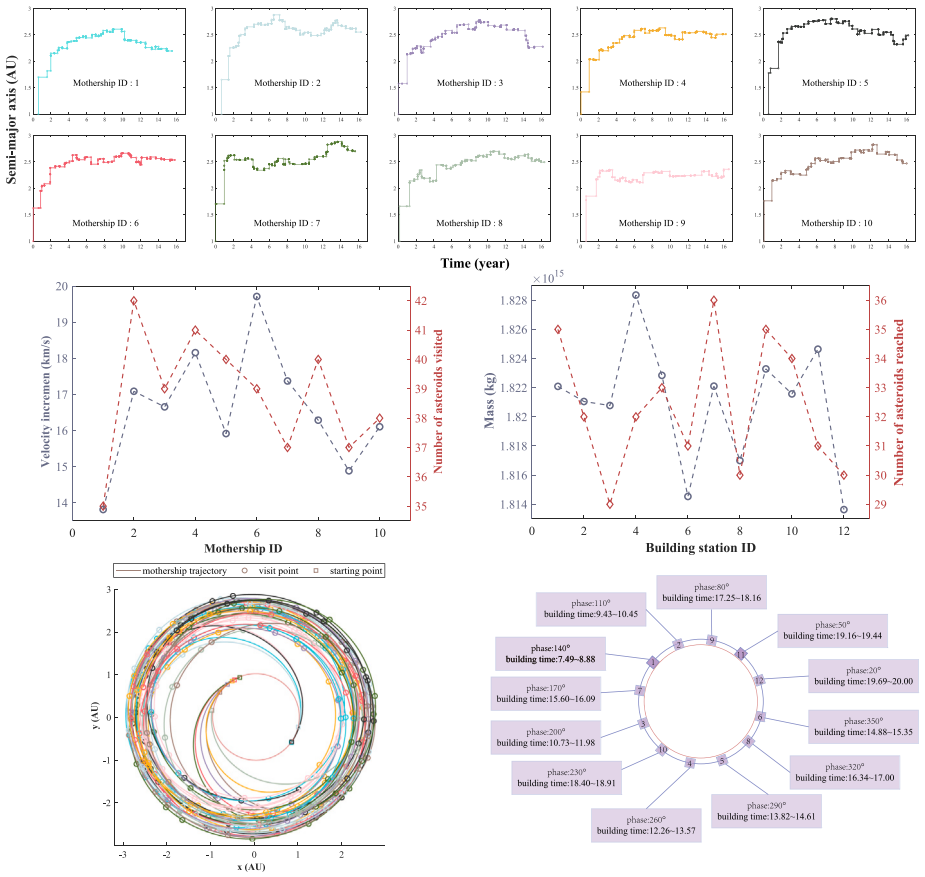


**Fig. 11.** Final result overview.

**Table 1**
Details of mothership trajectory of the winning result.

| ID | $T_k^s$ (MJD) | $n$ | $V_k$ (km/s) | Asteroids sequence |
|---|---|---|---|---|
| 1 | 95957.00501 | 35 | 13.81 | 74928 83061 82639 77508 83143 58218 66550 72752 81702 83047 59211 60832 83289 29268 57826 62130 60464 60742 82009 65656 44893 46577 75947 73100 83147 51745 55265 76542 83355 39257 82230 53541 82010 69347 45635 |
| 2 | 95980.29835 | 42 | 17.09 | 55311 74017 64405 78557 70679 82171 76482 82929 62379 78603 60163 55116 44688 83127 76822 54357 74712 83358 76543 81594 74131 83273 81089 80800 81314 81683 67096 81318 78422 63894 19108 78191 48818 53518 36883 78044 17062 74091 78291 54240 32559 78049 |
| 3 | 95757.55797 | 39 | 16.66 | 80044 60783 83310 66337 83095 66483 65860 75930 53659 82500 77262 81352 83192 42584 82566 64667 47806 55895 53231 80730 66332 66829 15280 48566 67448 16855 60885 49427 39987 82955 79842 52164 75762 81832 82933 57469 76335 81607 59026 |
| 4 | 95750.04584 | 41 | 18.16 | 80705 69772 66334 72693 60234 37539 82809 83152 50733 80698 83391 79539 67347 71440 70701 77569 47896 78858 53313 64426 36585 81821 80003 33479 82229 45710 39962 68729 83203 82044 54390 66541 80213 63509 47044 53789 77037 36382 78604 69072 79968 |
| 5 | 95958.24952 | 40 | 15.92 | 80069 80175 80925 58841 61681 81521 68246 69091 61716 49353 81875 22435 53150 74240 63717 83420 75691 55656 48563 37166 31826 58790 68166 63889 83024 79839 80789 67461 74686 27137 52916 75594 71253 68957 57626 80493 72016 77185 82164 73127 |
| 6 | 95746.52748 | 39 | 19.71 | 70432 81692 80282 65203 80321 64518 74833 76980 68984 83259 30205 40313 81848 14451 78178 82260 54457 64345 53223 56095 60790 70550 60744 63762 41518 72024 52222 76766 79384 72971 79312 54187 57818 68234 83184 77108 81982 61946 81951 |
| 7 | 95739.00000 | 37 | 17.37 | 77860 49741 72526 53021 40610 38476 54910 82987 81718 67684 83191 73733 43129 57576 64978 82907 82313 81490 81592 61809 82330 79990 81836 83290 77055 48582 81132 83351 70357 74978 51381 82949 80600 50808 77570 43770 82630 |
| 8 | 95798.62301 | 40 | 16.29 | 80735 65564 63816 82551 52265 29291 72843 83277 72666 67067 77814 74998 60309 81871 16137 83321 77847 83348 79237 77943 51275 40151 50709 81680 63372 50971 35695 72675 62162 81701 62360 81940 70452 74361 45267 48881 78055 75117 74966 81589 |
| 9 | 95958.72498 | 37 | 14.89 | 75508 82897 82349 81104 82484 74195 71832 55975 64880 42395 76824 63217 82722 74556 83255 78857 83346 82682 77717 59322 71257 64724 65895 80716 77718 73976 82953 74280 80747 71295 83256 76240 76929 83309 83190 83419 49893 |
| 10 | 95772.10462 | 38 | 16.10 | 61230 57026 67175 46652 81331 82869 26709 78391 79062 42658 81763 57129 80310 63313 83248 78628 43728 54395 71840 82763 69830 20376 47374 74063 31825 45579 80341 77723 11518 76649 78669 82959 74691 76623 83288 83340 82858 69120 |

**Table 2**
Results of top 10 teams.

| Team Rankings | 1 | 2 | 3 | 4 | 5 | 6 | 7 | 8 | 9 | 10 |
|---|---|---|---|---|---|---|---|---|---|---|
| Solution Detail | | | | | | | | | | |
| Dyson Ring semi-major axis $a$ (AU) | 1.10 | 1.32 | 1.05 | 1.10 | 1.09 | 1.30 | 1.10 | 1.40 | 1.10 | 1.00 |
| Dyson Ring inclination $i$ (deg) | 0.72 | 1.43 | 0.85 | 0.00 | 0.00 | 0.00 | 0.00 | 0.00 | 3.52 | 8.00 |
| Total number of the transferred asteroids $N$ | 388 | 301 | 293 | 235 | 209 | 346 | 250 | 294 | 213 | 199 |
| Average impulses per mothership $\Delta v$ (km/s) | 16.6 | 17.4 | 19.5 | 13.1 | 14.7 | 21.4 | 15.6 | 13.2 | 25.4 | 25.2 |
| Maximal mass $M_{\max}$ ($10^{15}$ kg) | 1.828 | 2.044 | 1.307 | 1.141 | 1.139 | 1.916 | 1.132 | 1.595 | 1.063 | 0.874 |
| Minimal mass $M_{\min}$ ($10^{15}$ kg) | 1.814 | 2.013 | 1.277 | 1.133 | 1.100 | 1.892 | 1.085 | 1.502 | 1.031 | 0.800 |
| [a]Theoretical upper bound of $M_{\min}$ ($10^{15}$ kg) | 1.929 | 2.220 | 1.450 | 1.281 | 1.248 | 2.302 | 1.325 | 1.920 | 1.216 | 0.997 |
| [a]Optimization efficiency of dividing station $\eta$ | 0.940 | 0.907 | 0.881 | 0.884 | 0.881 | 0.822 | 0.819 | 0.782 | 0.848 | 0.802 |
| Solution score | | | | | | | | | | |
| [a]Estimated score | 8211 | 6263 | 6188 | 5761 | 5294 | 6026 | 5725 | 5241 | 4010 | 3860 |
| Best score (from Leaderboard) | 8443 | 6359 | 5992 | 5885 | 5525 | 5487 | 5208 | 4794 | 3735 | 3532 |

[a]Calculated by the evaluation procedure from TsinghuaLAD&509.

## References


[1] H.X. Shen, Y.Z. Luo, Y.H. Zhu, A.Y. Huang, Dyson sphere building: On the design of the GTOC11 problem and summary of the results, Acta Astronaut. (2022) (this issue).

[2] A. Petropoulos, D. Grebow, D. Jones, G. Lantoine, A. Nicholas, J. Roa, J. Senent, J. Stuart, N. Arora, T. Pavlak, T. Lam, T. McElrath, R. Roncoli, D. Garza, N. Bradley, D. Landau, Z. Tarzi, F. Laipert, E. Bonfiglio, M. Wallace, J. Sims, GTOC9: Results from the jet propulsion laboratory (team JPL), Acta Futur. 11 (2018) 25–35, http://dx.doi.org/10.5281/zenodo.1139152.

[3] H.-X. Shen, T.-J. Zhang, A.-Y. Huang, Z. Li, GTOC 9: Results from the Xi'an satellite control center (team XSCC), Acta Futur. 11 (2018) 49–55, http://dx.doi.org/10.5281/zenodo.1139240.

[4] T.-J. Zhang, D. Wolz, H.-X. Shen, Y.-Z. Luo, Spanning tree trajectory optimization in the galaxy space, Astrodynamics 5 (1) (2021) 27–37, http://dx.doi.org/10.1007/s42064-020-0088-3.

[5] D. Wu, Y. Song, Z. Chi, Z. E, H. Sun, H. Baoyin, F. Jiang, Problem A of the 9th China trajectory optimization competition: Results found at Tsinghua university, Acta Astronaut. 150 (May) (2018) 204–212, http://dx.doi.org/10.1016/j.actaastro.2018.06.001.

[6] N. Zhang, Z. Zhang, H. Baoyin, Timeline club: An optimization algorithm for solving multiple debris removal missions of the time-dependent traveling salesman problem model, Astrodynamics (2021) http://dx.doi.org/10.1007/s42064-021-0107-z.

[7] S.G. Johnson, The Nlopt nonlinear-optimization package, 2014, URL http://github.com/stevengj/nlopt.

[8] T.H. Rowan, Functional Stability Analysis of Numerical Algorithms (Ph.D. thesis), The University of Texas at Austin, 1990, p. 218, Unpublished Dissertation.

[9] L.F. Simões, D. Izzo, E. Haasdijk, A.E. Eiben, Multi-rendezvous spacecraft trajectory optimization with beam P-ACO, in: Lecture Notes in Computer Science (Including Subseries Lecture Notes in Artificial Intelligence and Lecture Notes in Bioinformatics), vol. 10197 LNCS, 2017, pp. 141–156, http://dx.doi.org/10.1007/978-3-319-55453-2_10, arXiv:1704.00702.

[10] Z. Zhang, N. Zhang, Y. Jiao, H. Baoyin, J. Li, Multi-tree search for multi-satellite responsiveness scheduling considering orbital maneuvering, IEEE Trans. Aerosp. Electron. Syst. (2021) http://dx.doi.org/10.1109/TAES.2021.3129723.

[11] D. Wu, W. Wang, F. Jiang, J. Li, Minimum-time low-thrust many-revolution geocentric trajectories with analytical costates initialization, Aerosp. Sci. Technol. 119 (2021) 107146, http://dx.doi.org/10.1016/j.ast.2021.107146.

[12] J.L. Junkins, E. Taheri, Exploration of alternative state vector choices for low-thrust trajectory optimization, J. Guid. Control Dyn. 42 (1) (2019) 47–64, http://dx.doi.org/10.2514/1.G003686.

[13] F. Jiang, G. Tang, J. Li, Improving low-thrust trajectory optimization by adjoint estimation with shape-based path, J. Guid. Control Dyn. 40 (12) (2017) 3280–3287, http://dx.doi.org/10.2514/1.G002803.

[14] Y. Gao, C.A. Kluever, Low-thrust interplanetary orbit transfers using hybrid trajectory optimization method with multiple shooting, in: Collection of Technical Papers - AIAA/AAS Astrodynamics Specialist Conference, vol. 2, 2004, pp. 726–747, http://dx.doi.org/10.2514/6.2004-5088.

[15] F.L. Lewis, Optimal control, in: The Control Systems Handbook: Control System Advanced Methods, second ed., John Wiley & Sons, 2010, pp. 577–612, http://dx.doi.org/10.1201/b10384.

[16] F. Jiang, H. Baoyin, J. Li, Practical techniques for low-thrust trajectory optimization with homotopic approach, J. Guid. Control Dyn. 35 (1) (2012) 245–258, http://dx.doi.org/10.2514/1.52476.

[17] J.J. Moré, B.S. Garbow, K.E. Hillstrom, User Guide for MINPACK-1, Tech. Rep., CM-P00068642, 1980, URL http://www.netlib.org/minpack.

[18] T.N. Edelbaum, Propulsion requirements for controllable satellites, ARS J. 31 (8) (1961) 1079–1089, http://dx.doi.org/10.2514/8.5723.

[19] A.E. Petropoulos, J.M. Longuski, Shape-based algorithm for automated design of low-thrust, gravity-assist trajectories, J. Spacecr. Rockets 41 (5) (2004) 787–796, http://dx.doi.org/10.2514/1.13095.

[20] D. Wu, T. Zhang, Y. Zhong, F. Jiang, J. Li, Analytical shaping method for low-thrust rendezvous trajectory using cubic spline functions, Acta Astronaut. 193 (2022) 511–520, http://dx.doi.org/10.1016/j.actaastro.2022.01.019.

[21] D. Izzo, M. Märtens, B. Pan, A survey on artificial intelligence trends in spacecraft guidance dynamics and control, Astrodynamics 3 (4) (2019) 287–299, http://dx.doi.org/10.1007/s42064-018-0053-6.